

# THE DISTANCE TO AN X-RAY SHADOWING MOLECULAR CLOUD IN URSA MAJOR

ROBERT A. BENJAMIN,<sup>1</sup> KIM A. VENN,<sup>2</sup> DANIEL D. HILTGEN, AND CHRISTOPHER SNEDEN

Department of Astronomy, University of Texas at Austin, Austin, TX 78712; benjamin@halo.spa.umn.edu

Received 1995 February 23; accepted 1996 January 5

## ABSTRACT

We have obtained high-resolution optical spectra toward nine stars in the direction of a high-latitude, intermediate-velocity neutral cloud in Ursa Major in order to ascertain the distance to this complex. This cloud is of interest for several reasons. It is an infrared cirrus cloud, shows a distinct X-ray shadow, and turns out to be one of only three molecular clouds known to be well above the plane of the Galaxy. Interstellar Na I absorption is detected in four of the nine stars, but only the most distant star in our sample (BD +63°985) shows absorption at the velocity of the cloud as determined by the 21 cm and CO observations of Heiles, Reach, & Koo. We use several Fe I and Fe II stellar absorption features to determine the spectral type and luminosity class of the three most distant stars. Using the spectral type–absolute magnitude relationship from Schmidt-Kaler, and making no correction for extinction, we derive a distance to the cloud of  $d = 355 \pm 95$  pc, which corresponds to  $z = 285 \pm 75$  pc. Estimating the effects of extinction, we find that the true value could be as low as  $d = 240$  pc. This distance puts the cloud beyond the expected extent of the Local Bubble of hot ( $T \approx 10^6$  K) gas, showing that the X-ray emission behind this cloud arises in the Galactic halo. The cloud has dimensions  $\sim 15 \times 50$  pc, with a total estimated atomic mass of  $\sim 1600 M_\odot$ . The molecular mass of the cloud core, G135.3  $\pm$  54.5, is  $\sim 0.1 M_\odot$ .

*Subject headings:* ISM: clouds — ISM: individual (G135.3 + 54.5) — ISM: molecules — stars: distances — X-rays: ISM

## 1. INTRODUCTION

The *ROSAT* detection of X-ray shadows caused by neutral clouds between the solar system and areas of diffuse X-ray-emitting gas has opened up an important new approach for studying the interstellar medium (ISM). Using this technique, it has become possible to determine the three-dimensional structure of the hot component of the ISM and test various models for the origin of the diffuse soft X-ray background. In particular, these shadows allow us to determine if, and to what extent, X-ray emission comes primarily from a Local Bubble (see Cox & Reynolds 1987) of hot gas, assumed to extend 100–200 pc from the Sun, or from hot gas in a Galactic halo (see Spitzer 1990). Mapping the observed diffuse X-ray emission and correlating these results with structures seen in other wavelengths is necessary in order to piece together the hydrodynamical history of the interstellar medium in the region of the Sun.

A key ingredient in interpreting these data is the determination of the distances of the X-ray shadowing clouds. The most unambiguous method of determining the distance is to look for interstellar absorption due to the cloud in the spectra of stars of known distances. We have been successful in setting both upper and lower bounds on the distance to an X-ray shadowing cloud in Ursa Major (UMa). In § 2 we summarize what is known about this cloud. In § 3 we describe our observations and the results of our high-resolution optical spectroscopy, and in § 4 we use the distance to the cloud to draw some conclusions about the nature of the cloud and of the hot interstellar medium in this direction.

## 2. THE URSA MAJOR INTERMEDIATE-VELOCITY CLOUD

The UMa intermediate-velocity cloud (IVC) under consideration here is of interest for several reasons. As well as exhibiting an X-ray shadow, it is also a high-latitude molecular cloud, and has been detected in infrared emission using *IRAS*. In the following discussion, we summarize the results of previous studies of this region.

Snowden et al. (1994a) have surveyed the region around the cloud using the *ROSAT* PSPC in the  $\frac{1}{4}$  keV X-ray band ( $\sim 0.12$ – $0.284$  keV) and compared these results with maps of the 21 cm H I emission. Both maps used a similar angular resolution of 21'. Figure 1 shows the 21 cm map of the UMa IVC from this work, showing the column density of neutral hydrogen in the velocity range  $-75 \text{ km s}^{-1} < v_{\text{LSR}} < -25 \text{ km s}^{-1}$ . The locations of our target stars are also marked on this map. The cloud is located next to a region of low total H I column density (Lockman, Johoda, & McCammon 1986; Johoda, Lockman, & McCammon 1990) and compared to this region shows a distinct X-ray shadow. The low column density region with  $N(\text{H I}) \approx 0.8 \times 10^{20} \text{ cm}^{-2}$  has an X-ray count rate of  $I_X = (1200 \pm 30) \times 10^{-6} \text{ counts s}^{-1} \text{ arcmin}^{-2}$  in the  $\frac{1}{4}$  keV band. Contrastingly, in the direction of the cloud, which has a typical neutral hydrogen column density  $N(\text{H I}) \approx 2.0 \times 10^{20} \text{ cm}^{-2}$ , the X-ray count rate is 50% lower, with  $I_X = (670 \pm 20) \times 10^{-6} \text{ counts s}^{-1} \text{ arcmin}^{-2}$ .

Three sections of this cloud, designated G135.5 + 51.3, G137.3 + 53.9, and G135.3 + 54.5, have been selected for study by Heiles, Reach, & Koo (1988, hereafter HRK), who were attempting to compare the CO content, *IRAS* emission, and H I columns of isolated, degree-size clouds. As a result, G135.3 + 54.5 was discovered to be a member of the small class of high-latitude molecular clouds that have anomalous radial velocities (see Blitz 1991). The *IRAS* colors they determined for G135.3 + 54.5,  $I_{60}/I_{100} = 0.244$ ,

<sup>1</sup> Current address: Astronomy Department, University of Minnesota, 116 Church Street, SE, Minneapolis, MN 55455.

<sup>2</sup> Current address: Institut für Astronomie und Astrophysik, Scheinerstrasse 1, München, Germany, 81679.

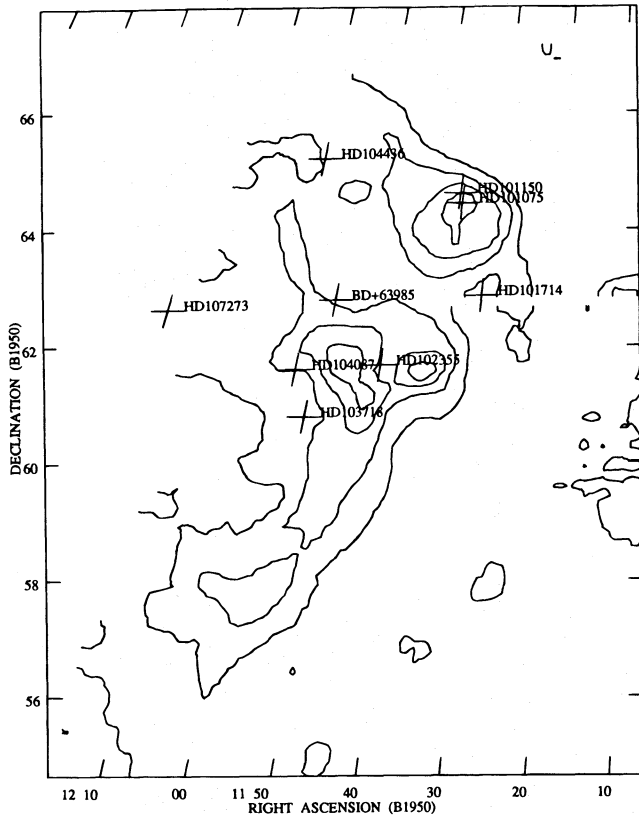


FIG. 1.—Map of  $N(\text{H I})$  in UMa intermediate-velocity cloud from Snowden et al. (1994a). Contour levels are  $N(\text{H I}) = 1.0, 1.5, 2.0, 2.5, 3.0 \times 10^{20} \text{ cm}^{-2}$ . The locations of our program stars are noted on the map.

$I_{25}/I_{100} = 0.120$ ,  $I_{12}/I_{100} = 0.036$ , with  $I_{100} = 1.64 \text{ MJy sr}^{-1}$ , are typical of clouds in this velocity range [ $v_{\text{LSR}}(\text{H I}) = -47.0 \text{ km s}^{-1}$ ;  $v_{\text{LSR}}(\text{CO}) = -45 \text{ km s}^{-1}$ ]. HRK measured the neutral hydrogen column density to be  $N(\text{H I}) = 1.28 \times 10^{20} \text{ cm}^{-2}$ , which disagrees with the  $\text{H I}$  column density of Snowden et al. (1994a) shown in Figure 1. HRK's column densities were obtained by taking the difference between on- and off-position observations, where the off position was  $1^\circ$  to the north. From Figure 1, we note that  $\text{H I}$  column density at the off-position observation was  $\sim 50\%$  of the on-position value, causing HRK to underestimate the total  $\text{H I}$  column; we thus believe the value should be revised upward to  $N(\text{H I}) = 2.2 \times 10^{20} \text{ cm}^{-2}$ .

There are two respects in which this cloud seems unusual. First, the presence of molecular gas, while consistent with the low internal velocity dispersion in this cloud,  $\Delta v_{\text{H I}} = 4.6$

$\text{km s}^{-1}$ , is unusual given the anomalous velocity of the cloud. With the exception of the Draco cloud (Goerigk et al. 1983), G211+63 (Désert, Bazell, & Blitz 1990), and this cloud, intermediate-velocity clouds are not observed to have a molecular component. Given its molecular component, the ratio  $I_{100}/N(\text{H I})$  for this cloud is also unusual. HRK have claimed that this ratio is a useful diagnostic for the evidence of molecular gas in a cloud. For purely atomic clouds, they found that  $I_{100}/N(\text{H I}) = 1.3 \text{ MJy sr}^{-1} 10^{-20} \text{ cm}^{-2}$ , while the same ratio for molecular clouds was higher, typically  $I_{100}/N(\text{H I}) \geq 2.5$ . For this cloud, using HRK's column estimate of  $N(\text{H I}) = 1.28 \times 10^{20} \text{ cm}^{-2}$ , one finds  $I_{100}/N(\text{H I}) = 1.28 \text{ MJy sr}^{-1} \times 10^{-20} \text{ cm}^{-2}$ , which is close to the ratio of 1.3 they obtained for purely atomic clouds. We find therefore that G135.3+54.5 does not show an infrared excess as expected for molecular clouds.

Finally, this cloud appears to be part of a large angular scale arch of  $\text{H I}$  that has been studied by Danly (1992), and thus is potentially part of a large-scale infall of neutral material in the northern Galactic hemisphere. Understanding the spatial and velocity structure of this intermediate-velocity arch is potentially important in understanding the disk-halo interaction in the Milky Way.

### 3. RESULTS

#### 3.1. Observations and Reductions

We have looked for evidence of interstellar  $\text{Na I}$  absorption at 5889.95 and 5895.92 Å in the spectra of nine stars in the direction of the UMa cloud (see Fig. 1). The basic stellar parameters are given in Table 1. These stars were observed either using the Sandiford Cassegrain echelle spectrograph on the 2.1 m reflector, or with the coude spectrograph on the 2.7 m reflector at McDonald Observatory. Both instruments were used with a spectral resolution of  $\sim 50,000$  at 5900 Å. Several hot (earlier than B2), rapidly rotating ( $v \sin i > 150 \text{ km s}^{-1}$ ) stars were observed and used to cancel telluric absorption features. For most cases, the atmospheric correction was done using the spectrum of  $\eta$  UMa ( $1 = 100^\circ 69$ ,  $b = +65^\circ 32$ ), which showed evidence of only very weak interstellar absorption at  $v_{\text{LSR}} = +14.7 \text{ km s}^{-1}$ . We experimented with different divisor stars and found we obtained nearly identical results. Wavelengths were calibrated with a Th-Ar lamp and checked using telluric features. The absolute wavelength calibration is accurate to  $\pm 0.03 \text{ Å}$ , or a velocity resolution of  $\pm 1.5 \text{ km s}^{-1}$ .

The resultant spectra corrected for atmospheric absorption and divided by a smooth fit to the continuum are shown in Figure 2, where the velocity scale was translated

TABLE 1  
STARS TOWARD URSA MAJOR CLOUD

Star	$\alpha_{2000}$	$\delta_{2000}$	$l$	$b$	Spectral Type <sup>a</sup>	$V$	$d_o$ (pc)	$d_R$ (pc)	$d_H$ (pc)	$z_o$ (pc)
HD 102355.....	11 <sup>h</sup> 47 <sup>m</sup> 08 <sup>s</sup> .0	+61°24'49"	135°99	54°07	F0 V	6.62	61 ± 10	61 ± 10	58 ± 10	49
HD 101150 <sup>b</sup> .....	11 38 49.0	+64 20 49	135.31	51.00	A5 IV	6.46	108 ± 15	108 ± 15	100 ± 15	84
HD 104436.....	12 01 37.6	+64 56 22	131.07	51.71	A3 V	7.27	143 ± 20	108 ± 15	139 ± 20	112
HD 104087.....	11 59 15.5	+61 20 04	133.73	54.69	A3 V	7.6	166 ± 25	166 ± 25	160 ± 25	135
HD 107273.....	12 19 40.1	+62 21 32	129.25	54.38	A3 V	7.8	182 ± 25	112 ± 15	179 ± 25	148
HD 103718.....	11 56 43.9	+60 31 20	134.74	55.33	A3 V	8.0	200 ± 30	123 ± 20	192 ± 30	164
HD 101714.....	11 42 41.0	+62 35 00	135.93	52.78	A7 IV	9.1	302 ± 40	164 ± 30	295 ± 60	240
HD 101075.....	11 38 22.3	+64 10 36	135.50	51.13	A2 IV	7.9	240 ± 35	191 ± 30	223 ± 35	187
BD +63°985.....	11 55 24.1	+62 31 04	133.74	53.42	A5 V	9.9	389 ± 60	266 ± 60	374 ± 60	312

<sup>a</sup> See text for discussion of spectral classification.

<sup>b</sup> Double star; see McAlister et al. 1989.

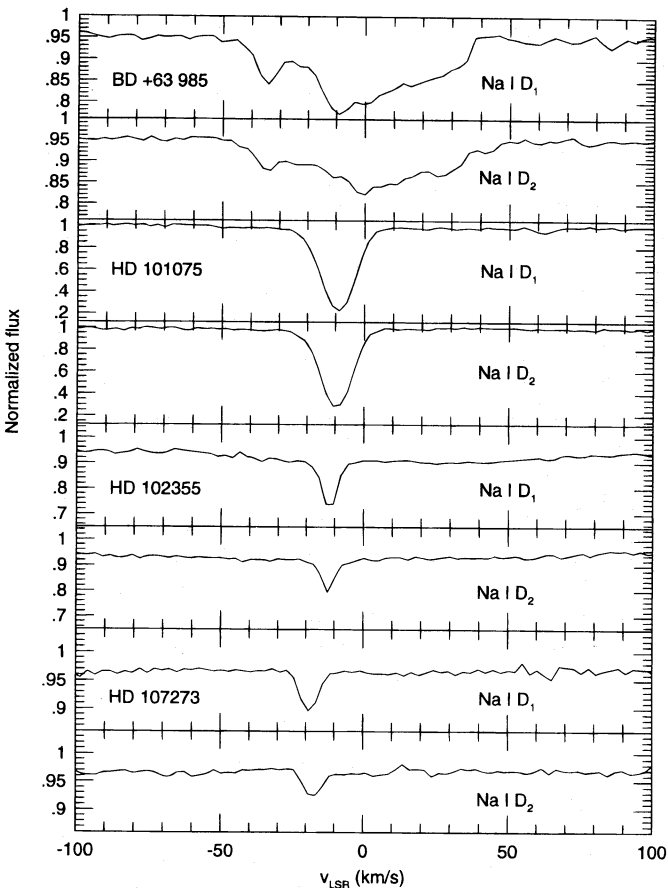


FIG. 2.—Plots of detected Na I absorption detected in four of our program stars. HD 101075, HD 102355, and HD 107273 all show absorption at  $-10\text{ km s}^{-1}$  to  $-20\text{ km s}^{-1}$ . BD +63°985 shows broad stellar features centered at  $-20\text{ km s}^{-1}$ , but also a clear interstellar absorption line at  $-47\text{ km s}^{-1}$ .

to the local standard of rest reference frame ( $v_{\text{LSR}}$ ). We consider a feature a true detection if absorption is observed in both Na I lines, and the measured velocities agree to within  $1\text{ km s}^{-1}$  ( $0.02\text{ \AA}$ ). Where possible, the equivalent widths of both components are measured. The results are given in Table 2. Although four stars in our sample show evidence of interstellar Na I absorption, only the most distance star in our sample, BD +63°985, shows evidence for absorption at the velocity of the cloud. The measured velocity,  $v_{\text{LSR}} = -44.9 \pm 0.7\text{ km s}^{-1}$ , is in good agreement with the H I ( $v_{\text{LSR}} = -47\text{ km s}^{-1}$ ) and CO detections ( $v_{\text{LSR}} = -45\text{ km s}^{-1}$ ) measured by HRK for G135.3+54.5. This absorption feature was observed at the same heliocentric velocity in both June and July, despite a shift of  $4\text{ km s}^{-1}$  between June and July due to the Earth’s motion, thus eliminating the possibility that it is telluric in origin and making it less likely that it is a transient stellar feature. The spectra for both epochs along with the star used for atmospheric division are shown in Figure 3.

### 3.2. The Distance to the Cloud

The distances to our target stars given in Table 1 are calculated from the star’s spectral type and the spectral type–absolute magnitude relation of Schmidt-Kaler (1982). No luminosity classes have been determined for our target stars (see SIMBAD database). We assume they are all dwarf stars, but for the three stars most important in constraining the cloud distance we determine the stellar properties from a classical model atmospheres analysis. Distances are then determined by comparing the absolute magnitudes to the observed magnitudes. Assuming no error in the spectral class of the stars, this distance should be accurate to within 15%. The principal source of uncertainty in measuring the distance comes from the uncertainty of 0.3 mag in the absolute magnitude calibration (see Schmidt-Kaler 1982 and references therein). These distances, uncorrected for the effects of interstellar extinction, are given as  $d_0$  in Table 1. The corresponding vertical distances from the Galactic mid-plane are given as  $z_0$ .

We make two estimates for the extinction correction. First, we calculate the color excess  $E_{B-V} = (B-V) - (B-V)_0$  for each star using  $B$  and  $V$  values from the SIMBAD database, and taking the intrinsic color from Schmidt-Kaler (1982). This is converted to visual extinction assuming  $A_V/E_{B-V} = 3.2$  (Mathis 1990). Although this value of  $A_V/E_{B-V}$  is determined for disk gas, and a lower value may apply in the halo, it is sufficient to provide a rough estimate of the extinction. The resulting distances are given in Table 1 as  $d_R$ . For those stars with a negative color excess, we set  $A_V = 0$ . Since small uncertainties in the relative values of  $B$  and  $V$  translate into large uncertainties in the extinction correction (except for HD 102355 and HD 104436, for which more accurate photometry was available), these values are useful only in estimating the possible effects of extinction. For our second extinction estimate, we take the total H I column density and assume the standard relation  $\langle N(\text{H I})/E_{B-V} \rangle = 4.93 \times 10^{21}\text{ cm}^{-2}\text{ mag}^{-1}$  (Diplas & Savage 1993). Since some fraction of the 21 cm emission

TABLE 2  
DETECTED INTERSTELLAR Na I ABSORPTION LINES

Star	Date Observed (UT)	S/N	$v_{\text{LSR}}$ (km s <sup>-1</sup> )	EW $D_1$ (mÅ)	EW $D_2$ (mÅ)
HD 102355.....	1993 Mar 14.3	170	$-12.0 \pm 0.5$	31	15.2
HD 101150.....	1993 Mar 14.2	120	...	...	...
HD 104436.....	1993 Jul 05.2	110	...	...	...
HD 104087.....	1993 Mar 14.4	60	...	...	...
HD 107273.....	1993 May 05.2	220	$-17.1 \pm 0.4$	11.2	6.5
HD 103718.....	1993 Jun 14.1	100	...	...	...
HD 101714.....	1993 Jun 14.1	60	...	...	...
HD 101075.....	1993 Mar 14.3	130	$-9.9 \pm 0.3$	227	190
BD +63°985.....	1993 Jun 12.1	70	$-44.9 \pm 0.7^a$	20	9.7
	1993 Jul 05.2	130	...	...	...

<sup>a</sup> Absorption feature too blended with broad stellar feature to allow reliable measurement of equivalent width.



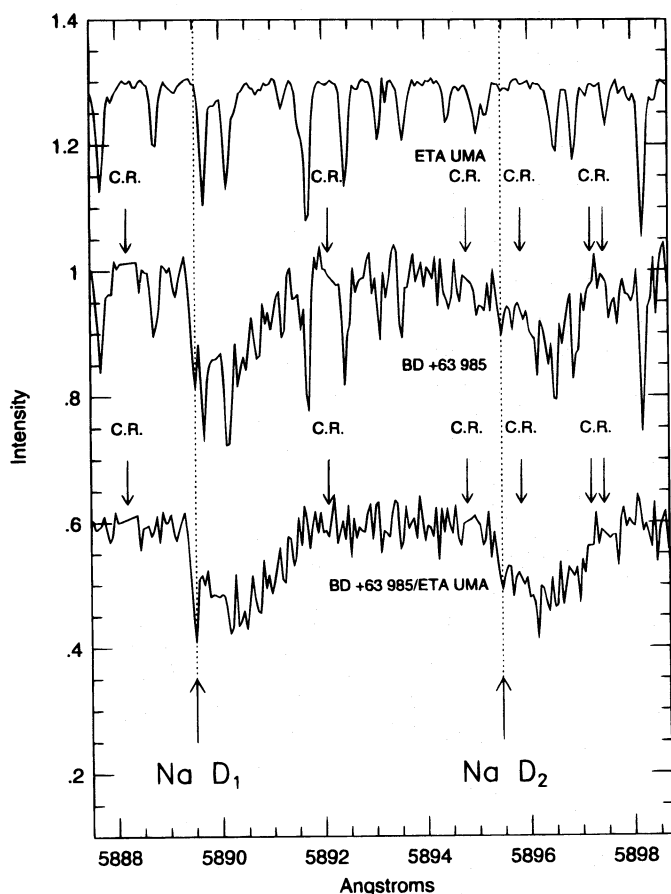


FIG. 3a

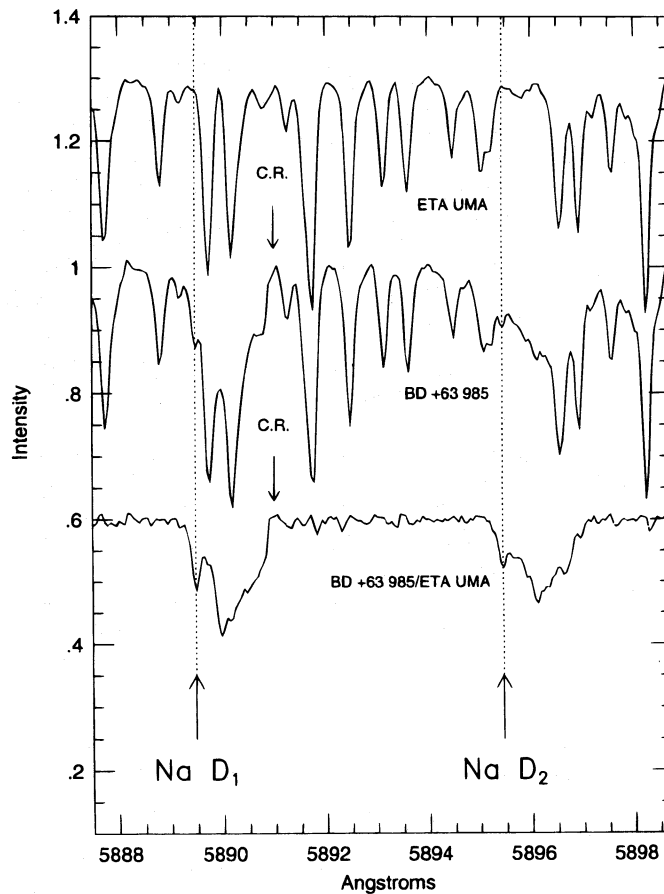


FIG. 3b

FIG. 3.—(a) Detection of interstellar Na I absorption in the spectrum of BD + 63°985 taken on 1993 June 12. Top spectra is that of  $\eta$  UMa, the star used to divide out telluric features in the spectrum of BD + 63°985. The interstellar feature is marked with a dotted line. Also noted are the locations of cosmic-ray spikes removed during data reduction. (b) Same as (a), but for spectra taken on 1993 July 5.

used to estimate the total H I column densities may arise in gas beyond the stars, this value should be an upper limit, and the distance corrected for this value,  $d_H$ , is actually a lower limit. However, we find that the extinction estimated by using the  $N(\text{H I})$  measurements is significantly less than that using the color excess. This is probably due to the fact that there is some additional extinction due to refractory elements in the ionized gas along the path length to the cloud. Pending accurate photometry for these stars, we will use the distances uncorrected for extinction, but note that the distances to the three farthest stars in our sample could conceivably decrease by as much as 120 pc.

The three most important stars for bracketing the distance to the cloud are the background star BD + 63°985, which sets the upper limit on the cloud distance, and the two most distant foreground stars, HD 101075 and HD 101714, which provide the lower limit. [Although it is possible that these two stars lie behind holes in a patchy distribution of Na I, the fact that there are two such stars makes this seem less likely. Moreover, the column density of  $N(\text{H I})$  in the direction of HD 101075 is a factor of 1.8 higher than that toward BD + 63°985; therefore, it seems less likely to lie in a hole.] While we have not obtained low-resolution spectra to reclassify these stars, we have checked to see whether the stellar features observed in our high-resolution spectra are consistent with the assumed spectral classifications, or whether modification of the spectral types

is necessary. For each of these three stars, we measured the equivalent widths of several stellar absorption lines of Fe I and Fe II (typically about 10 lines of each ionization species). An LTE model atmospheres analysis of these features using Kurucz ATLAS9 models (Kurucz 1979, 1991) gives the following stellar parameters: HD 101714,  $T_{\text{eff}} = 7800 \pm 400$  K,  $\log g = 3.5 \pm 0.3$ ,  $\zeta$  (micro-turbulence)  $= 4 \pm 1$  km s $^{-1}$ , and  $[\text{Fe}] = 0.0 \pm 0.2$ ; HD 101075,  $T_{\text{eff}} = 9000 \pm 400$  K,  $\log g = 3.5 \pm 0.4$ ,  $\zeta = 3 \pm 1$  km s $^{-1}$ , and  $[\text{Fe}] = 0.2 \pm 0.2$ ; BD + 63°985,  $T_{\text{eff}} = 8200 \pm 400$  K,  $\log g = 4.2 \pm 0.4$ ,  $\zeta = 2 \pm 1$  km s $^{-1}$ ,  $[\text{Fe}] = 0.0 \pm 0.2$ . Using these parameters, we have estimated the luminosity classes, and modified the spectral types. These revised spectral types are listed in Table 1. With these accurate temperatures and surface gravities, uncertainty in the spectral classification is no longer a major source of uncertainty in the final distance estimates.

Using the distances derived for the background star, BD + 63°985 ( $d = 389 \pm 60$  pc), and the most distant foreground star, HD 101714 ( $d = 302 \pm 40$  pc), we estimate a distance to the cloud of  $d = 355 \pm 95$  pc, where the uncertainty in this distance comes from the range of uncertainty in the distances to the two bracketing stars. We note, however, that taking into account corrections for extinction could lower this distance to a value as low as  $\sim 240$  pc. For the following analysis, we use the 355 pc value as the best estimate of the cloud distance.

## 4. IMPLICATIONS

## 4.1. X-Ray Emitting Gas in the Halo

The most important result of this study is the demonstration that an appreciable fraction of the X-ray emission seen in this direction arises at a distance greater than 300 pc above the Galactic plane, outside the main Galactic H I layer. This complements the Draco cloud results of Burrows & Mendenhall (1991) and Snowden et al. (1991), adding further evidence that there is  $T \approx 10^6$  K gas in the Galactic halo as would be expected in the Galactic fountain model of Shapiro & Field (1976). Unlike the Draco cloud distance determination of Lilienthal et al. (1991), however, we are able to place both a lower *and* an upper bound on the distance to the cloud, which greatly simplifies interpretation of the X-ray shadow results. Snowden et al. (1994a) find that the unattenuated halo X-ray flux from beyond the UMa cloud is only 13% of the intensity calculated to arise behind the Draco cloud. This indicates that the distribution of hot gas in the halo is inhomogeneous. The extent of the inhomogeneity and an understanding of the physical origin of the heated regions of the halo await the distance determination and analysis of additional X-ray shadowing clouds.

## 4.2. Local X-Ray Emission

This distance determination also allows us to assess the physical parameters of the hot interstellar material in the foreground of the cloud. We have calculated the soft X-ray emission of a gas in the temperature range  $T_0 = 10^{6.0}-10^{6.2}$  K using the cosmic chemical abundances of Grevesse & Anders (1989), and atomic data from Raymond & Smith (1977) and Raymond (1987). The resultant emergent intensity is then multiplied by the *ROSAT* PSPC effective area curve (Snowden et al. 1994b), and converted to a  $\frac{1}{4}$  keV intensity for comparison with *ROSAT* data. Matching our calculated intensity to the observed X-ray emission in the direction of the cloud,  $I_x = 695 \times 10^{-6}$  counts s $^{-1}$  arcmin $^{-2}$ , yields an emission measure for the gas between us and the cloud of  $EM_{\text{front}} = 4-5 \times 10^{-3}$  cm $^{-6}$  pc. If we assume that the path length between Earth and the cloud is filled with a uniform-density constant-temperature gas, our distance estimate to the cloud allows us to derive an average density for the X-ray-emitting gas of  $n_H = 3-4 \times 10^{-3}$  cm $^{-3}$ . If only the fraction  $f$  of the path length is occupied by X-ray-emitting gas, then the density estimate will increase by a factor  $f^{-1/2}$  or more, since the intervening noncoronal gas will introduce some absorption.

## 4.3. Physical Parameters of the Cloud

Our distance determination is also useful for constraining fundamental parameters of the cloud itself. The mass of a cloud is given by

$$M_{H\text{I}} = 3 M_{\odot} \left( \frac{N(\text{H I})}{10^{20} \text{ cm}^{-2}} \right) \left( \frac{\Omega}{1 \text{ deg}^2} \right) \left( \frac{d}{100 \text{ pc}} \right)^2.$$

The entire UMa cloud complex has a filamentary appear-

ance, extending roughly  $2^\circ \times 8^\circ$ . At the distance derived in this paper, this would correspond in linear dimensions to  $\sim 13 \text{ pc} \times 53 \text{ pc}$ . Assuming a mean column density  $N(\text{H I}) = 2 \times 10^{20} \text{ cm}^{-2}$  yield a mass estimate for the atomic component of the total complex of  $\sim 1600 M_{\odot}$ . The radius and mass of the atomic components of the cloud cores observed by HRK are as follows: G135.5+51.3,  $R = 4 \text{ pc}$ ,  $M = 30 M_{\odot}$ ; G137.3+53.9,  $R = 5 \text{ pc}$ ,  $M = 50 M_{\odot}$ ; G135.3+54.5,  $R = 5 \text{ pc}$ ,  $M = 50 M_{\odot}$ . This does not include the molecular gas also in the cloud. According to Reach, Koo, & Heiles (1994), the CO line integral is  $W(\text{CO}) = 0.9 \text{ K km s}^{-1}$ , and the CO emission is limited to a region with an effective angular diameter  $\theta_D = 4'$ . Assuming a CO-to-H $_2$  conversion factor of  $x_{\text{WCO}} = N(\text{H}_2)/W(\text{CO}) = 0.5 \times 10^{20} \text{ cm}^{-2} (\text{K km s}^{-1})^{-1}$  (de Vries, Heithausen, & Thaddeus 1987), we derive  $M_{\text{H}_2} = 0.1 M_{\odot}$ . Since there is a large range of variation in the conversion factor  $x_{\text{WCO}}$  from  $0.02 \times 10^{20}$  (Herbstmeier, Heithausen, & Mebold 1993) to  $2.3 \times 10^{20}$  (Bloemen, Deul, & Thaddeus 1990), the mass estimate is similarly uncertain. In all cases, we find that these masses are less than the virial masses, and thus the clumps are not self-gravitating.

## 4.4. Future Directions

In this work, we have shown how accurate distance determinations to interstellar structures can provide important information, allowing us to derive physical parameters for the cloud and the surrounding interstellar medium. We have shown that the UMa IVC cloud is located in the low Galactic halo, that X-ray-emitting gas is located at even greater distances, and that the cloud can serve as probe of the physical conditions in the Galactic halo. Moreover, we have identified a background source (BD +63°985) which in the future can be exploited to learn about the chemical process occurring in this molecular cloud along this particular line of sight. We expect that future studies planned for other interstellar structures should yield similarly interesting and useful results.

R. A. B. would like to thank P. Shapiro for helpful discussions and encouragement during the course of this work, and H. Dinerstein and the referee for helpful comments on the manuscript. We would also like to thank D. McCammon, W. Sanders, M. Juda, and D. Burrows for providing information on the X-ray shadowing cloud candidate; W. Reach for useful discussion on the CO and H I observations; J. C. Howk and F. J. Lockman for supplying the H I map used in Figure 1; and D. Hines for assistance in preparing Figure 1. We also thank J. Krelowski for obtaining observations of two target stars, and M. Hanson and B. E. Penprase for their advice in selecting some of the target stars. This research has made use of the SIMBAD database, operated at CDS, Strasbourg, France, and was supported by NASA grant NGT-50849 as well as by funds from McDonald Observatory.

## REFERENCES

- Blitz, L. 1991, in *Molecular Clouds*, ed. R. A. James & T. J. Millar (Cambridge: Cambridge Univ. Press), 49  
 Bloemen, J. B. G. M., Deul, E. R., & Thaddeus, P. 1990, *A&A*, 233, 437  
 Burrows, D. N., & Mendenhall, J. A. 1991, *Nature*, 351, 629  
 Cox, D. P., & Reynolds, R. J. 1987, *ARA&A*, 25, 303  
 Danly, L. 1992, *PASP*, 104, 819  
 Désert, F.-X., Bazell, D., & Blitz, L. 1990, *ApJ*, 355, L51  
 de Vries, H. W., Heithausen, A., & Thaddeus, P. 1987, *ApJ*, 319, 723  
 Diplas, A., & Savage, B. D. 1994, *ApJ*, 427, 274  
 Goerigk, W., Mebold, U., Reif, K., Kalberla, P. M. W., & Velden, L. 1983, *A&A*, 120, 63  
 Grevesse, N., & Anders, E. 1989, in *Cosmic Abundances of Matter*, ed. C. J. Waddington (New York: AIP), 183  
 Heiles, C., Reach, W. T., & Koo, B.-C. 1988, *ApJ*, 332, 313 (HRK)

- Herbstmeier, U., Heithausen, A., & Mebold, U. 1993, *A&A*, 272, 514  
Jahoda, K., Lockman, F. J., & McCammon, D. 1990, *ApJ*, 354, 184  
Kurucz, R. L. 1979, *ApJS*, 40, 1  
———. 1991, private communication  
Lilienthal, D., Wennmacher, A., Herbstmeier, U., & Mebold, U. 1991, *A&A*, 250, 150  
Lockman, F. J., Johoda, K., & McCammon, D. 1986, *ApJ*, 302, 432  
Mathis, J. S. 1990, *ARA&A*, 28, 37  
McAlister, H. A., Hartkopf, W. I., Sowell, J. R., Dombrowski, E. G., & Franz, O. G. 1989, *AJ*, 97, 510  
Raymond, J. C. 1987, private communication  
Raymond, J. C., & Smith, B. W. 1977, *ApJS*, 35, 419  
Reach, W. T., Koo, B.-C., & Heiles, C. 1994, *ApJ*, 429, 672  
Schmidt-Kaler, T. 1982, in *New Ser.*, VI, Vol. 2b, *Stars and Star Clusters*, ed. Landolt-Bornstein (Berlin: Springer), 18  
Shapiro, P. R., & Field, G. B. 1976, *ApJ*, 205, 762  
Snowden, S. L., Hasinger, G., Jahoda, K., Lockman, F. J., McCammon, D., & Sanders, W. T. 1994a, *ApJ*, 430, 601  
Snowden, S. L., McCammon, D., Burrows, D. N., & Mendenhall, J. A. 1994b, *ApJ*, 424, 714  
Snowden, S. L., Mebold, U., Hirth, W., Herbstmeier, U., & Schmitt, J. H. M. M. 1991, *Science*, 252, 1529  
Spitzer, L. 1990, *ARA&A*, 28, 71